

Computed tomography–based radiomics modeling to predict patient overall survival in cervical cancer with intensity-modulated radiotherapy combined with concurrent chemotherapy

Lihong Xiao¹ , Youhua Wang²,
Xiangxiang Shi¹, Haowen Pang¹ and Yunfei Li¹

Abstract

Objective: The objective of this study was to develop a predictive model combining radiomic characteristics and clinical features to forecast overall survival in cervical cancer patients treated with intensity-modulated radiotherapy and concurrent chemotherapy.

Methods: In this retrospective observational study, 159 patients were divided into a training group (n = 95) and a validation group (n = 64). Radiomic characteristics were extracted from contrast-enhanced computed tomography scans. The least absolute shrinkage and selection operator regression analysis was used to filter the extracted radiomic characteristics and reduce the dimensionality of the data. A radiomic score was calculated from the selected features, and multivariate Cox regression models were established to analyze overall survival. A nomogram combining radiomic score and clinical features was developed, and its reliability was assessed using the area under the receiver operating characteristic curve.

Results: Four radiomic characteristics and two clinical features were extracted for overall survival analysis. A nomogram combining these factors was developed and validated, showing good performance with a high C-index. Patients were categorized as low-risk or high-risk for overall survival based on a cut-off value.

Corresponding authors:

Yunfei Li, Department of Oncology, The Affiliated Hospital of Southwest Medical University, Luzhou, Sichuan 646000, China.

Email: 1003401784@qq.com

Haowen Pang, Department of Oncology, The Affiliated Hospital of Southwest Medical University, Luzhou, Sichuan 646000, China.

Email: panghaowen1022@swmu.edu.cn

¹Department of Oncology, The Affiliated Hospital of Southwest Medical University, Luzhou, Sichuan, China

²Department of Oncology, Gulin County People's Hospital, Luzhou, Sichuan, China



Creative Commons Non Commercial CC BY-NC: This article is distributed under the terms of the Creative

Commons Attribution-NonCommercial 4.0 License (<https://creativecommons.org/licenses/by-nc/4.0/>) which permits non-commercial use, reproduction and distribution of the work without further permission provided the original work is attributed as specified on the SAGE and Open Access pages (<https://us.sagepub.com/en-us/nam/open-access-at-sage>).

Conclusions: Our model combining computed tomography–extracted radiomic characteristics and clinical features shows good potential for evaluating overall survival in cervical cancer patients treated with intensity-modulated radiotherapy and concurrent chemotherapy.

Keywords

Uterine cervical neoplasms, radiotherapy, intensity-modulated, drug therapy, computed tomography, prediction model

Date received: 20 November 2024; accepted: 19 February 2025

Introduction

Cervical cancer is the fourth most common type of cancer diagnosed in women and the fourth most common cause of cancer-related deaths in women. In fact, in 2018, there were an estimated 570,000 new cases of cervical cancer and 311,000 cervical cancer deaths globally.¹ The incidence and death rates of cervical cancer are the highest in Africa and Southeast Asian countries, which are 10 times that of Western countries.² In recent years, intensity-modulated radiotherapy (IMRT) has become one of the most important methods for the treatment of advanced cervical cancer.^{3,4} Several studies have reported that IMRT is an effective method for the treatment of advanced cervical cancer with acceptable toxicity.^{5–9} Advancements in radiotherapy treatment equipment and enhancements in irradiation technology have led to an increase in the survival rate of cervical cancer patients. However, even with these advancements, using currently available treatment methods, approximately 30%–50% of patients still experience treatment failures. Local recurrence has been identified as the main cause of failure, with distant metastasis occurring in approximately 15% of the patients.¹⁰ Therefore, in the context of advocating for precision medicine, predicting the OS of cervical cancer patients is of great significance for judging

prognosis and developing individualized treatment plans.

Radiomics is a newly developed field that has gained traction in recent years. It uses a large number of automated algorithms to extract data features and transform image data into data distributed in a high-dimensional feature space that is easy to analyze.^{11,12} Radiomics has developed rapidly and has already been applied to the diagnosis, treatment, and prediction of some tumors, including lung, rectal, prostate, and esophageal cancers.^{13–16} At present, many reports have pointed out that the extraction of radiomics parameters based on CT, magnetic resonance imaging (MRI), or positron emission tomography-computed tomography (PET-CT) images and the construction of a model can help analyze and predict pelvic lymph node metastasis in cervical cancer.^{17–24} It has also been reported that an MRI-based radiomics model can predict the efficacy of chemoradiotherapy for patients with locally advanced cervical cancers.^{25,26} For example, Lucia et al.^{27,28} reported that PET-CT and MRI radiomics models could be used to predict the prognosis and recurrence of cervical cancer in patients after chemoradiotherapy. However, few studies have focused on CT radiomics models to predict local control (LC) rates and OS after chemoradiotherapy in patients with cervical cancer. Therefore, our study

aimed to develop two models combining radiomic characteristics and clinical features that may be able to predict OS in patients with IMRT-treated cervical cancer, respectively.

Methods

Patient selection

In total, 159 cervical cancer patients treated at the Affiliated Hospital of Southwest Medical University between May 2012 and March 2020 were included in the retrospective study and randomly divided into the training and validation cohorts at a ratio of 6:4. This study was performed in compliance with the Helsinki Declaration of 1975, as revised in 2024. Ethical approval for this retrospective data analysis was obtained on 18 January 2021 from the Clinical Trial Ethics Committee of the Affiliated Hospital of Southwest Medical University (KY2021023), and the reporting of this study conforms to STROBE guidelines.²⁹ All patient details have been de-identified to protect individual privacy in accordance with ethical standards and relevant guidelines. Our study obtained written informed consent from all patients. After obtaining ethical approval and informed consent from participants, we accessed the data from 20 April 2021 to 27 September 2021. The inclusion criteria were as follows: (a) patients with cervical cancer confirmed by biopsy (according to the American Joint Committee on Cancer [AJCC], stages IB to IVA); (b) pre-treatment contrast-enhanced CT images available; (c) clinical data, including age, date of diagnosis, histology and Fédération Internationale de Gynécologie et d'Obstétrique (FIGO) stage, available; (d) no other treatment administered; and (e) satisfactory basic physical condition of the patient (Karnofsky score >70, age 18–70 years). Exclusion criteria included the following: (a) patients with concurrent other

malignant tumors; (b) incomplete or poor-quality data; (c) prior treatment with surgery, radiotherapy or chemotherapy before starting IMRT and concurrent chemotherapy; (d) poor general condition: Karnofsky performance status ≤ 70 or age not between 18 and 70 years; (e) pregnant or breastfeeding women at the start of treatment; (f) severe cognitive impairment or mental illness that prevents understanding and adhering to study requirements and treatment protocols; (g) autoimmune diseases or other conditions requiring long-term use of immunosuppressive agents; and (h) ethical concerns or refusal to participate by the patient or their family.

All patients underwent complete IMRT treatment. The doses of external beam radiotherapy were 45–50 Gy/25–28 fractions; radiotherapy was administered once a day, five times a week, for approximately 5 weeks, and IMRT plans were generated using the Pinnacle 8.0-m (Philips, Fitchburg, WI) treatment planning system. Treatment was delivered using a Varian 6EX accelerator (Varian Medical Systems, Palo Alto, California, USA) with a 6-MV photon beam. The doses of brachytherapy were 28–30 Gy/4–6 fractions; the initial prescription dose of clinical high-risk target was 6 Gy/fraction, 1–2 fractions/week. Brachytherapy was performed on an Ir192-source (mHDR, Elekta, Holland) with a micro-Selectron v3 Afterloader (Elekta, Holland). Patients received concurrent cisplatin chemotherapy of approximately 4–5 fractions once per week. In this study, the patients were treated with radiotherapy using extracorporeal radiation therapy combined with brachytherapy. In the choice of brachytherapy modality, intracorporeal radiotherapy was used for patients with more confined tumor locations and smaller sizes; intracorporeal plus intertissue cannula radiotherapy was used for patients with larger tumors or complex locations. In terms of dose calculation, the doses of

external irradiation and brachytherapy were calculated separately in this study, and the total dose of gross tumor volume (GTV) was derived by the superposition method.

Clinical endpoints and follow-up

After treatment completion, all patients were monitored every 3 months during the first 2 years, every 6 months for the next 3 years, and annually thereafter. The follow-up time was defined as the time from therapy initiation to the day of the last examination or death. We collected the clinicopathological characteristics of each patient including the age at diagnosis, FIGO stage, tumor histology, tumor response, radiotherapy dose, and pelvic lymph node metastasis status.

Image acquisition

All images used for radiomics analysis were obtained from radiotherapy-localized CT scans prior to IMRT. The same CT scanner was used for all patients, and all image acquisition and reconstruction parameters were the same for all patients. Contrast-enhanced CT scans were performed using a LightSpeed RT 4 scanner (GE Healthcare, Chicago, Illinois, USA). The scanning parameters used in this study were as follows: tube voltage, 120 kVp; field of view, 250–400 mm; pixel size, 512×512 ; slice thickness, 0.25 cm; and average number of slices, 116. The GTV region was segmented by two radiation oncologists with >10 years of clinical experience. In case of disagreement, it was referred to a third radiation oncologist with >15 years of clinical experience for judgment. GTV was directly delineated from the target area in radiotherapy-localized CT using MRI fusion. The MRI sequences used are T2-weighted imaging sequence (T2WI), diffusion-weighted imaging sequence. Dynamic contrast-enhanced MRI (DCE-MRI) is able to provide information

about tumor angiogenesis and perfusion by injecting a contrast agent and scanning it continuously, which helps characterize the tumor more fully. Organ mobility is a major concern during positioning and treatment, and we ask the patient to empty the rectum and fill the bladder and intravaginal markers in the same way. To prevent patient positional movement, we use somatic membrane immobilization. The radiomics features helpful for IMRT planning were extracted from the GTV using a three-dimensional (3D) slicer platform.

Statistical analyses

The statistical analyses of all data were completed using R software, version 4.4.0 (R Foundation for Statistical Computing, Vienna, Austria).

The least absolute shrinkage and selection operator (LASSO) regression analysis was used to select the radiomic characteristics (the “GLMNet” software package in R software), and the most valuable predicted radiomic characteristics were selected from the GTV to fit the Cox proportional model.

Multivariate Cox regression hazards models were used to establish the LC and OS prediction models for cervical cancer based on the selected radiomic characteristics and clinical characteristics, and the final results were presented through a nomogram. The above process and calibration curves were completed by the “survival” and “rms” packages in R software, respectively.

The area under the receiver operating characteristic curve (AUC) was used to evaluate the performance of the nomogram model. Each patient’s radiomic scores (rad-scores) were calculated by selecting a linear combination of radiomic characteristics and weighted by their respective partial regression coefficients.

Results

Clinical data

Table 1 summarizes the clinical data of the patients. At the time of analysis, the median follow-up time was 46 months (range: 0–92 months). There were 72 (75.8%) and 49 (76.6%) patients still alive at the time of the current analysis in training and validation cohorts. We selected tumor response after 1 month of radiotherapy, age, pathological stage, pelvic lymph node metastasis, Karnofsky performance status (KPS), and hemoglobin, white blood cells, neutrophils, lymphocytes, monocytes, and platelets before treatment as clinical characteristics. These clinical characteristics were screened

by proportional hazards model (Table 2). Finally, we screened out two clinical characteristics, the stage before treatment and the tumor response 1 month after IMRT, for subsequent modeling and analysis.

Radiomic signature building

A total of 851 radiomics features were extracted from the GTV, including shape features, first-order features, gray level dependence matrix (GLDM), gray level co-occurrence matrix (GLCM), neighboring gray tone difference matrix (NGTDM), gray level size zone matrix (GLSZM), and gray level run length matrix (GLRLM). LASSO regression was used to reduce the dimensionality of the extracted radiomics

Table 1. Characteristics of the patients at baseline.

| Characteristic | All patients (N = 159) No. (%) or median (range) |
|--|---|
| Age, y | 54 (43–70) |
| Karnofsky performance status | |
| 90 | 90 (57) |
| 80 | 67 (42) |
| 70 | 2 (1) |
| Neoplasm staging | |
| IB | 1 (1) |
| IIA | 20 (13) |
| IIB | 102 (64) |
| IIIA | 10 (6) |
| IIIB | 24 (15) |
| IVA | 2 (1) |
| Pelvic lymph node metastasis | |
| Positive | 33 (21) |
| Negative | 126 (79) |
| Curative effect evaluation after 1 month of radiotherapy | |
| CR | 135 (85) |
| PR | 18 (12) |
| PD | 2 (1) |
| SD | 4 (2) |
| Leukocyte (G/L, normal range: 3.5–5.5) | 6.6 (1.98–20.63) |
| Neutrophil (G/L, normal range: 1.8–6.3) | 4.01 (0.95–16.15) |
| Lymphocyte (G/L, normal range: 1.1–3.2) | 1.67 (0.33–3.44) |
| Monocyte (G/L, normal range: 0.1–0.6) | 0.38 (0.07–1.06) |
| Platelet (G/L, normal range: 125–350) | 272 (75–508) |
| HGB (g/L, normal range: 115–150) | 118 (55–149) |

CR: complete response; HGB: hemoglobin; PD: progressive disease; PR: partial response; SD: stable disease.

features and filter out the optimal radiomics features to predict OS (Figure 1). In the establishment of OS prediction model in the training cohort, four radiomics features were selected, including a maximum 2D diameter slice of the original shape (feature 1), skewness of the wavelet-LLH of the first order (feature 2), large area

high gray-level emphasis of the wavelet-LLH of the GLSZM (feature 3), and large area high gray-level emphasis of the wavelet-HLH of the GLSZM (feature 4). Calculate the rad-score based on the partial regression coefficients of the LASSO regression model. In the predictive analysis modeling of OS, four radiomic characteristics and two clinical features were extracted from the analysis, and their multivariate Cox regression hazards results were shown in Table 3. We divided the patients into low-risk and high-risk groups based on the rad-score (Figure 2), and the cut-off value was 0.17.

Table 2. Univariate Cox regression hazards.

| Covariate | <i>P</i> value | |
|----------------------------------|-----------------------|--------|
| Curative effect evaluation after | | |
| I month of radiotherapy | | |
| CR | | <0.001 |
| PR | 5.889 (2.169, 15.980) | <0.001 |
| SD/PD | 17.127 (6.921–42.38) | |
| Neoplasm staging | | |
| I/II | | |
| III/IV | 2.508 (1.135–5.540) | 0.023 |
| Age | 0.982 (0.935–1.032) | 0.476 |
| HGB | 0.998 (0.977–1.019) | 0.856 |
| KPS | 0.967 (0.899–1.041) | 0.375 |
| Pelvic lymph node metastasis | 1.486 (0.597–3.701) | 0.395 |
| Leukocyte | 0.999 (0.854–1.168) | 0.928 |
| Neutrophil | 1.027 (0.862–1.223) | 0.769 |
| Lymphocyte | 0.836 (0.417–1.678) | 0.614 |
| Monocyte | 0.499 (0.037–6.679) | 0.599 |
| Platelet | 3.433 (0.376–31.330) | 0.274 |

CR: complete response; HGB: hemoglobin; KPS: Karnofsky performance status; PD: progressive disease; PR: partial response; SD: stable disease.

Table 3. The results of the multivariate analysis.

| Covariate | P value | |
|--|-----------------------|--------|
| Curative effect evaluation after 1 month of radiotherapy | | |
| CR | | <0.001 |
| PR | 5.178 (1.838–14.585) | 0.002 |
| SD/PD | 10.723 (3.719–30.916) | |
| Neoplasm staging | | |
| I/II | | |
| III/IV | 1.781 (0.764–4.154) | 0.018 |
| rad-score | 1.740 (1.120–2.704) | 0.014 |

CR: complete response; PD: progressive disease; PR: partial response; rad-score: radiomic score; SD: stable disease.

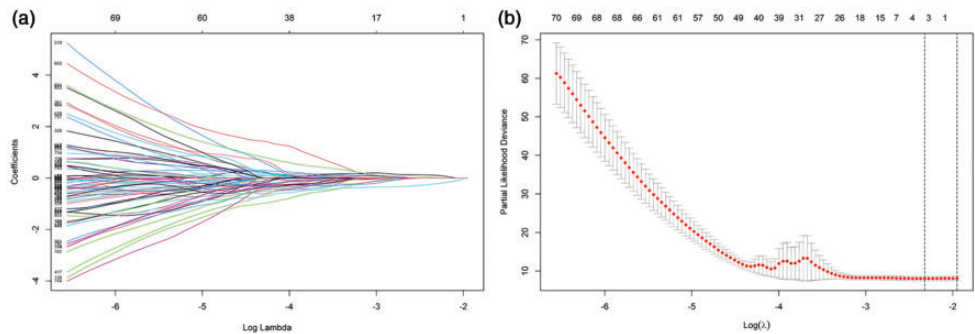


Figure 1. (a) is LASSO coefficient profiles of the 851 texture features in the LASSO model and (b) is 10-fold cross-validation with minimum criteria, used for the selection of the tuning parameter (λ). LASSO: least absolute shrinkage and selection operator.

Establishment of nomograms

The clinical characteristic nomogram and the combined clinical characteristic and rad-score nomogram are shown in Figure 3. The calibration curves of the validation cohort are shown in Figure 4.

Prediction performance of the nomogram models

The AUC curve representing the clinical characteristic and the combined clinical

characteristic and rad-score of the validation cohort are in Figure 5. For the AUC values of the validation cohort, they are 0.900 (0.734, 1.000), 0.790 (0.659, 0.920), and 0.803 (0.675, 0.931) for 1 year, 3 years, and 5 years, respectively. The AUC value of the combined clinical characteristic and rad-score model is higher than that of the clinical characteristic model alone. This proves that the predictive model combined with radiomic features and clinical characteristics may effectively improve the predictive performance.

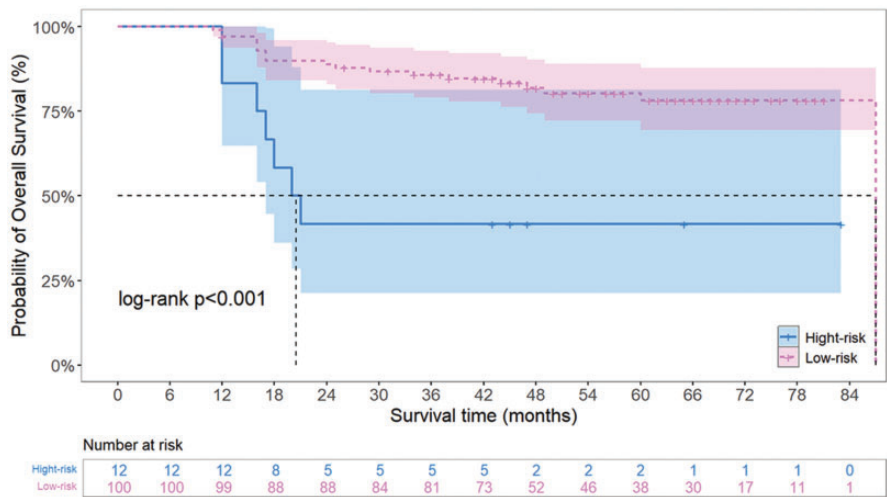


Figure 2. Kaplan–Meier curves for risk group stratification based on rad-score.

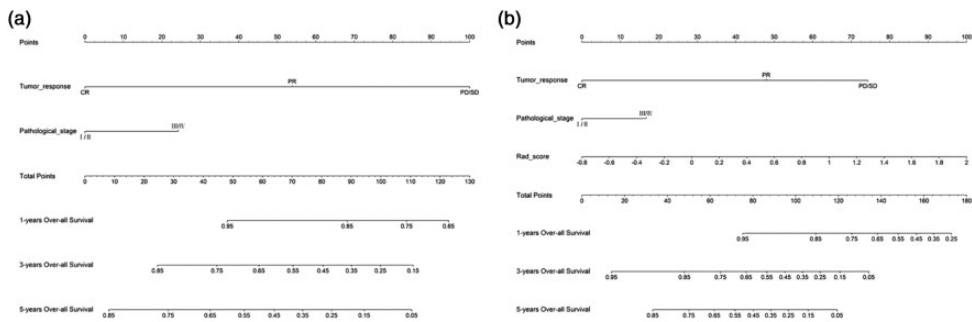


Figure 3. The clinical characteristic nomogram and the combined clinical characteristic and rad-score nomogram. A is the clinical characteristic nomogram; B is the combined clinical characteristic and rad-score nomogram.

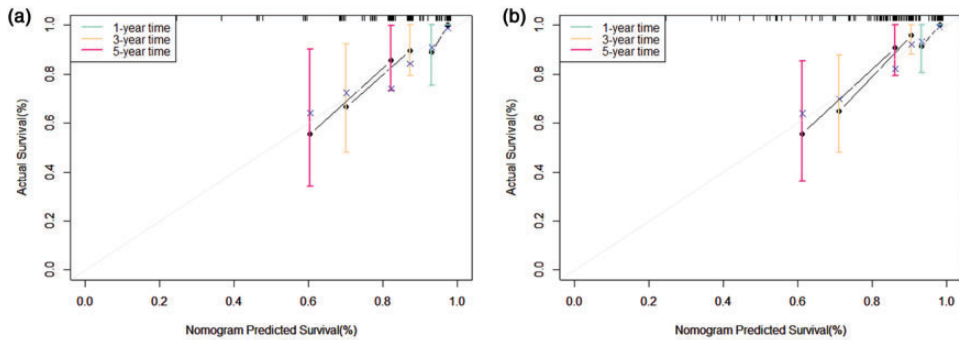


Figure 4. The calibration curves of the validation cohort. (a) is the calibration curve based on clinical characteristics and (b) is the calibration curve based on the combination of clinical characteristics and rad-score.

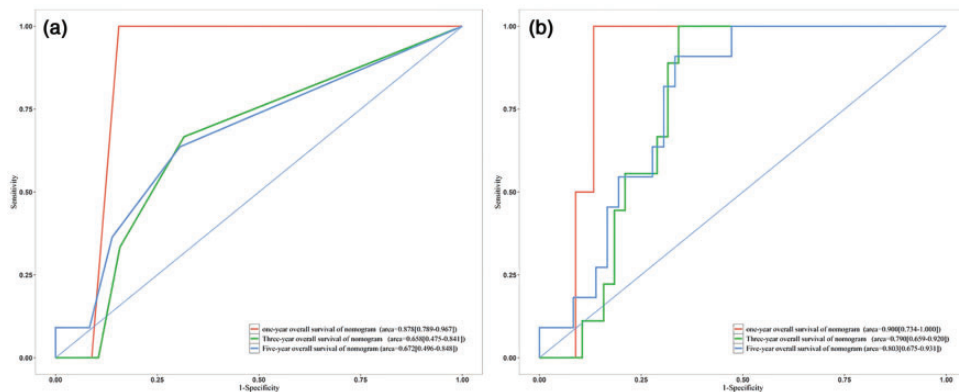


Figure 5. The AUC curve representing the clinical characteristic and the combined clinical characteristic and rad-score of the validation cohort. AUC: area under the receiver operating characteristic curve.

Discussion

Radiomics is an emerging research tool that has been used to assess tumor heterogeneity and prognosis, to some extent, by extracting high-throughput image features from images of different modes.³⁰ In cervical cancer, the application of radiomics has been widely reported, such as using CT, MRI and PET-CT radiomic characteristics to predict pelvic lymph node metastasis,^{17–24} [18F] fluorodeoxyglucose-PET radiomics to predict disease-free survival,³¹ and MRI scans to predict the efficacy of neoadjuvant chemoradiotherapy for advanced cervical

cancer.^{25,26} Taken together, these results demonstrate that the application of radiomics in the diagnosis and curative effect prediction of cervical cancer is reliable.

Previous radiomics models combining PET and MRI have been developed to predict recurrence in patients with cervical cancer undergoing radiotherapy and chemotherapy.²⁸ To date, there have been no reports of CT radiomics being used to predict the OS of cervical cancer. Although CT is less effective than MRI in soft tissue recognition and less effective than PET-CT in tumor metabolism and systemic metastasis determination, CT is more advantageous in

terms of cost and convenience. In this study, we developed a nomograph model combining radiomic characteristics and clinical features to predict OS in patients with cervical cancer receiving IMRT concurrent with chemotherapy. In the construction of clinical models, we selected tumor response after 1 month of radiotherapy, age, pathological stage, pelvic lymph node metastasis, KPS, and hemoglobin, white blood cells, neutrophils, lymphocytes, monocytes, and platelets before treatment as clinical characteristics. We selected some pre-treatment blood indicators for analysis because it has been reported that some blood indicators, such as hemoglobin, are closely associated with OS of cervical cancer.^{32,33} Through Cox regression hazards, the stage before treatment and the tumor response 1 month after IMRT were selected for subsequent analysis of OS prediction. This is consistent with the factors we think are associated with OS in clinical practice.

In the analysis of the radiomic feature extracted, all radiomic features screened using LASSO regression were correlated with the tumor response after 1 month of radiotherapy and with tumor staging. This does not mean, however, that the performance of models that combine clinical features and radiomic characteristics seems to be solely related to the clinical features we extract. Both the tumor response after 1 month of radiotherapy and the clinical stage are judgments made by clinicians after analyzing several simple factors such as tumor size, lymph node metastasis and distant organ metastasis, and are subjective to a certain extent. In some cases, different doctors may even make very different judgments. However, radiomic characteristics can avoid these problems, and they contain a lot of high-throughput information that clinicians cannot obtain with the naked eyes. Therefore, we believe that the information provided by clinical features is

included in the radiomic characteristics. By analyzing the AUC value, whether it was in the training cohort or the validation cohort, we demonstrate that the prediction model combining clinical features and the rad-score performs better than the model using clinical features alone and the model using the rad-score alone. This proves that our previous inference, the addition of radiomic characteristics, does improve the performance of the predictive model on the basis of the clinical model, the high performance of the combined model is not solely determined by clinical features. This demonstrates that CT-based radiomics provides valuable information that can reflect the biological behavior of the tumor, and radiomic characteristics and clinical features can effectively complement each other. In particular, when we extracted the radiomics features, we used the target area of the radiotherapy-localized CT delineated by the physician. Not only did we not need to spend extra time outlining the region of interest but also the target area was more consistent with our treatment area.

A previous study by Hanna et al.³⁴ reported that concurrent chemotherapy can provide additional benefits for patients. Another study by Mendz et al.³⁵ reported that in brachytherapy for cervical cancer, tumor patients with a low total dose of radiotherapy had a low OS, which seemed to be related to the dose delivered to the tumor. By using predictive models of radiomics in combination with patients' clinical characteristics, we may be able to predict the outcome of treatment at an early stage of treatment, alter the dose or modality of radiotherapy or allow additional therapy to be administered to patients who are likely to experience treatment failure, including performing surgical intervention when possible or additional targeted therapy. Patients were successfully classified into high-risk and low-risk groups based on the rad-score. This helps accurately stratify

patients in clinical practice as well as develop individualized treatment strategies. The rad-score, constructed from radiomic features, is a commonly used method for prognostic prediction in cervical cancer. Fang et al.³⁶ constructed a rad-score using MRI radiomic features and evaluated its relationship with predicting disease-free survival (DFS) in early-stage cervical cancer patients, confirming that the rad-score can serve as an accurate pre-treatment prognostic biomarker for predicting cervical cancer DFS. Zhang et al.³⁷ built a rad-score based on MRI radiomic features to predict the prognosis of locally advanced cervical squamous cell carcinoma patients receiving concurrent chemoradiotherapy, confirming the predictive value of the rad-score in forecasting treatment response and survival. Therefore, it can be observed that the rad-score constructed from radiomic features has good generalizability in the field of cervical cancer prognosis. This study confirms this characteristic in predicting the prognosis of cervical cancer patients receiving IMRT.

The LASSO regression model is a linear model used to estimate sparse parameters, which has a good effect on reducing the number of parameters and has a wide application in the field of compressed sensing.³⁸ In fact, a previous study by Yin et al.³⁹ compared the three feature selection methods of relief, random forest, and LASSO and found that LASSO had the best performance in the application of radiomics methods. Therefore, it was appropriate to select LASSO as the method for selecting radiomics features in this study.

This study has some limitations. First, pelvic lymph node metastasis of cervical cancer is closely related to recurrence and prognosis in patients, and many studies have discussed them in parallel.^{40–42} For example, Ayhan et al.⁴³ reported that adjuvant radiotherapy in stage IB cervical cancer patients with negative nodes does

not provide better local tumor control. Furthermore, early-stage node-positive cervical cancers are associated with local failure.^{44–47} In addition, histological type, as an essential part of cervical cancer, has been reported to be closely related to the prognosis of cervical cancer.^{33,48,49} Among cervical cancer, squamous cell carcinoma is the most common histological type of pathology. In this retrospective analysis, the histological type of most of our collected cases was squamous cell carcinoma, and only one case was non-squamous cell carcinoma; hence, we did not include this factor. In this study, only GTV was used as a reference when extracting the radiomics features, without the supplemental use of lymph node GTV. We plan to add lymph node GTV and histological type to our prediction model and explore the use of deep learning techniques for feature selection and modeling in future studies in an attempt to increase the judgment accuracy of the prognosis of cervical cancer patients. Additionally, genomic characteristics were not considered, and in recent years, genetic markers have been used to predict OS in patients with cervical cancer in research settings.⁵⁰ Radiogenomics has gradually emerged in the field of cancer research and has been reported in renal cell carcinoma, colorectal cancer, glioblastoma, and other cancers.^{51,52} Therefore, more patients needed to be included in studies to identify relevant genetic characteristics and accurately predict OS in patients. Third, as a retrospective analysis, some patients had different treatment baselines, and future studies should standardize the treatment methods to minimize the influence of other factors on the results.

Conclusion

This study shows that the combination of CT-extracted radiomic characteristics and clinical features has promising potential

for evaluating OS in patients with cervical cancer who underwent chemoradiotherapy.

Abbreviations

| | |
|--------|---|
| 3D | three-dimensional |
| AJCC | American Joint Committee on Cancer |
| AUC | area under the receiver operating characteristic curve |
| CT | Contrast-Enhanced computed tomography |
| FIGO | Fédération Internationale de Gynécologie et d'Obstétrique |
| GLCM | gray level co-occurrence matrix |
| GLDM | gray level dependence matrix |
| GLRLM | gray level run length matrix |
| GLSZM | gray level size zone matrix |
| GTV | gross tumor volume |
| HGB | hemoglobin |
| IMRT | intensity-modulated radiotherapy |
| KPS | Karnofsky performance status |
| LASSO | least absolute shrinkage and selection operator |
| LC | local control |
| NGTDM | neighboring gray tone difference matrix |
| OS | overall survival |
| PET-CT | positron emission tomography-computed tomography |

Acknowledgements

We sincerely thank all patients who participated in this study. Your support and trust made this study possible. At the same time, we would also like to thank the Affiliated Hospital of Southwest Medical University for providing a valuable platform and the support of the above-mentioned funds.

Author contributions

Haowen Pang and Yunfei Li: guarantor of integrity of entire study. Lihong Xiao and Xiangxiang Shi: literature research. Yunfei Li, Lihong Xiao, and Youhua Wang: statistical analysis and

manuscript editing. All authors: study concepts, study design, data acquisition, data analysis and interpretation, manuscript drafting and manuscript revision for important intellectual content, approval of final version of submitted manuscript, agree to ensure any questions related to the work are appropriately resolved, and clinical studies.

Data availability statement

The datasets generated and analyzed during this study contain sensitive patient information and are not publicly available to protect patient privacy and confidentiality. These data were collected with approval from the Clinical Trial Ethics Committee of the Affiliated Hospital of Southwest Medical University and informed consent from all participants. Researchers interested in accessing the data should contact the corresponding author. Access will be granted subject to institutional review board approval and compliance with ethical guidelines.

Declaration of conflicting interests

The authors declare that there is no conflict of interest.

Ethics statement

This study involves human participants. Treatment and data analyses were conducted in accordance with the Declaration of Helsinki. Ethical approval for this retrospective data analysis was obtained from the Clinical Trial Ethics Committee of the Affiliated Hospital of Southwest Medical University (KY2021023).

Funding

The Gulin County People's Hospital-The Affiliated Hospital of Southwest Medical University Science and Technology Strategic Cooperation Project (project number: 2022GLXNYDFY05); The Xuyong County People's Hospital-Southwest Medical University Science and Technology Strategic Cooperation Project (project number: 2024XYXNYD05); Sichuan Medical and Health Care Promotion Institute Project (project number: KY2022SJ 0377); Radiation Oncology Key Laboratory of Sichuan Province Project (project number:

2024ROKF01); The Southwest Medical University Foundation (project number: 2020ZRQNA033).

ORCID iD

Lihong Xiao  <https://orcid.org/0000-0002-7111-1299>

References

- De Martel C, Plummer M, Vignat J, et al. Worldwide burden of cancer attributable to HPV by site, country and HPV type. *Int J Cancer* 2017; 141: 664–670.
- Bray F, Ferlay J, Soerjomataram I, et al. Global cancer statistics 2018: GLOBOCAN estimates of incidence and mortality worldwide for 36 cancers in 185 countries. *CA Cancer J Clin* 2018; 68: 394–424.
- Meng Q, Liu X, Hu K, et al. Image-guided intensity-modulated radiotherapy in patients with FIGO IIIC1 cervical cancer: efficacy, toxicity and prognosis. *J Cancer* 2023; 14: 1001–1010.
- Lin Y, Chen K, Lu Z, et al. Intensity-modulated radiation therapy for definitive treatment of cervical cancer: a meta-analysis. *Radiat Oncol* 2018; 13: 177.
- Chang Y, Yang ZY, Li GL, et al. Correlations between radiation dose in bone marrow and hematological toxicity in patients with cervical cancer: a comparison of 3DCRT, IMRT, and RapidARC. *Int J Gynecol Cancer* 2016; 26: 770–776.
- Contreras J, Srivastava A, Chundury A, et al. Long-term outcomes of intensity-modulated radiation therapy (IMRT) and high dose rate brachytherapy as adjuvant therapy after radical hysterectomy for cervical cancer. *Int J Gynecol Cancer* 2020; 30: 1157–1161.
- Dang YZ, Li P, Li JP, et al. Efficacy and toxicity of IMRT-based simultaneous integrated boost for the definitive management of positive lymph nodes in patients with cervical cancer. *J Cancer* 2019; 10: 1103–1109.
- Lei C, Ma S, Huang M, et al. Long-term survival and late toxicity associated with pelvic intensity modulated radiation therapy (IMRT) for cervical cancer involving CT-based positive lymph nodes. *Front Oncol* 2019; 9: 520.
- Wang X, Shen Y, Zhao Y, et al. Adjuvant intensity-modulated radiotherapy (IMRT) with concurrent paclitaxel and cisplatin in cervical cancer patients with high risk factors: a phase II trial. *Eur J Surg Oncol* 2015; 41: 1082–1088.
- Hasselle MD, Rose BS, Kochanski JD, et al. Clinical outcomes of intensity-modulated pelvic radiation therapy for carcinoma of the cervix. *Int J Radiat Oncol Biol Phys* 2011; 80: 1436–1445.
- Kumar V, Gu Y, Basu S, et al. Radiomics: the process and the challenges. *Magn Reson Imaging* 2012; 30: 1234–1248.
- Lambin P, Rios-Velazquez E, Leijenaar R, et al. Radiomics: extracting more information from medical images using advanced feature analysis. *Eur j Cancer* 2012; 48: 441–446.
- Delli Pizzi A, Chiarelli AM, Chiacchiaretta P, et al. MRI-based clinical-radiomics model predicts tumor response before treatment in locally advanced rectal cancer. *Sci Rep* 2021; 11: 5379.
- Li M, Yang L, Yue Y, et al. Use of radiomics to improve diagnostic performance of PI-RADS v2.1 in prostate cancer. *Front Oncol* 2020; 10: 631831.
- Li Y, Liu J, Li HX, et al. Radiomics signature facilitates organ-saving strategy in patients with esophageal squamous cell cancer receiving neoadjuvant chemoradiotherapy. *Front Oncol* 2020; 10: 615167.
- Yan M and Wang W. A radiomics model of predicting tumor volume change of patients with stage III non-small cell lung cancer after radiotherapy. *Sci Prog* 2021; 104: 36850421997295.
- Chen X, Liu W, Thai TC, et al. Developing a new radiomics-based CT image marker to detect lymph node metastasis among cervical cancer patients. *Comput Methods Programs Biomed* 2020; 197: 105759.
- Deng X, Liu M, Sun J, et al. Feasibility of MRI-based radiomics features for predicting lymph node metastases and VEGF expression in cervical cancer. *Eur J Radiol* 2021; 134: 109429.

19. Hou L, Zhou W, Ren J, et al. Radiomics analysis of multiparametric MRI for the pre-operative prediction of lymph node metastasis in cervical cancer. *Front Oncol* 2020; 10: 1393.
20. Li XR, Jin JJ, Yu Y, et al. PET-CT radiomics by integrating primary tumor and peritumoral areas predicts E-cadherin expression and correlates with pelvic lymph node metastasis in early-stage cervical cancer. *Eur Radiol* 2021; 31: 5967–5979.
21. Song J, Hu Q, Ma Z, et al. Feasibility of T2WI-MRI-based radiomics nomogram for predicting normal-sized pelvic lymph node metastasis in cervical cancer patients. *Eur Radiol* 2021; 31: 6938–6948.
22. Wang T, Gao T, Yang J, et al. Preoperative prediction of pelvic lymph nodes metastasis in early-stage cervical cancer using radiomics nomogram developed based on T2-weighted MRI and diffusion-weighted imaging. *Eur J Radiol* 2019; 114: 128–135.
23. Wu Q, Wang S, Chen X, et al. Radiomics analysis of magnetic resonance imaging improves diagnostic performance of lymph node metastasis in patients with cervical cancer. *Radiother Oncol* 2019; 138: 141–148.
24. Xiao M, Ma F, Li Y, et al. Multiparametric MRI-based radiomics nomogram for predicting lymph node metastasis in early-stage cervical cancer. *J Magn Reson Imaging* 2020; 52: 885–896.
25. Fang M, Kan Y, Dong D, et al. Multi-habitat based radiomics for the prediction of treatment response to concurrent chemotherapy and radiation therapy in locally advanced cervical cancer. *Front Oncol* 2020; 10: 563.
26. Liu D, Zhang X, Zheng T, et al. Optimisation and evaluation of the random forest model in the efficacy prediction of chemoradiotherapy for advanced cervical cancer based on radiomics signature from high-resolution T2 weighted images. *Arch Gynecol Obstet* 2021; 303: 811–820.
27. Lucia F, Visvikis D, Desseroit MC, et al. Prediction of outcome using pretreatment 18F-FDG PET/CT and MRI radiomics in locally advanced cervical cancer treated with chemoradiotherapy. *Eur J Nucl Med Mol Imaging* 2018; 45: 768–786.
28. Lucia F, Visvikis D, Vallières M, et al. External validation of a combined PET and MRI radiomics model for prediction of recurrence in cervical cancer patients treated with chemoradiotherapy. *Eur J Nucl Med Mol Imaging* 2019; 46: 864–877.
29. Von Elm E, Altman DG, Egger M; STROBE Initiative, et al. The Strengthening the Reporting of Observational Studies in Epidemiology (STROBE) statement: guidelines for reporting observational studies. *Ann Intern Med* 2007; 147: 573–577.
30. Lambin P, Leijenaar RTH, Deist TM, et al. Radiomics: the bridge between medical imaging and personalized medicine. *Nat Rev Clin Oncol* 2017; 14: 749–762.
31. Ferreira M, Lovinfosse P, Hermesse J, et al. [18F]FDG PET radiomics to predict disease-free survival in cervical cancer: a multi-scanner/center study with external validation. *Eur J Nucl Med Mol Imaging* 2021; 48: 3432–3443.
32. Khalil J, El Kacemi H, Afif M, et al. Five years' experience treating locally advanced cervical cancer with concurrent chemoradiotherapy: results from a single institution. *Arch Gynecol Obstet* 2015; 292: 1091–1099.
33. Yalman D, Aras AB, Ozkök S, et al. Prognostic factors in definitive radiotherapy of uterine cervical cancer. *Eur J Gynaecol Oncol* 2003; 24: 309–314.
34. Hanna TP, Shafiq J, Delaney GP, et al. The population benefit of radiotherapy for cervical cancer: local control and survival estimates for optimally utilized radiotherapy and chemoradiation. *Radiother Oncol* 2015; 114: 389–394.
35. Mendez LC, Weiss Y, D'Souza D, et al. Three-dimensional-guided perineal-based interstitial brachytherapy in cervical cancer: a systematic review of technique, local control and toxicities. *Radiother Oncol* 2017; 123: 312–318.
36. Fang J, Zhang B, Wang S, et al. Association of MRI-derived radiomic biomarker with disease-free survival in patients with early-stage cervical cancer. *Theranostics* 2020; 10: 2284–2292.
37. Zhang X, Zhao J, Zhang Q, et al. MRI-based radiomics value for predicting the survival of patients with locally advanced

- cervical squamous cell cancer treated with concurrent chemoradiotherapy. *Cancer Imaging* 2022; 22: 35.
38. Gui J and Li H. Penalized Cox regression analysis in the high-dimensional and low-sample size settings, with applications to microarray gene expression data. *Bioinformatics* 2005; 21: 3001–3008.
 39. Yin P, Mao N, Zhao C, et al. Comparison of radiomics machine-learning classifiers and feature selection for differentiation of sacral chordoma and sacral giant cell tumour based on 3D computed tomography features. *Eur Radiol* 2019; 29: 1841–1847.
 40. Niu C, Sun X, Zhang W, et al. NR2F6 expression correlates with pelvic lymph node metastasis and poor prognosis in early-stage cervical cancer. *Int J Mol Sci* 2016; 17: 1694.
 41. Yang S, Liu Y, Xia B, et al. DLL4 as a predictor of pelvic lymph node metastasis and a novel prognostic biomarker in patients with early-stage cervical cancer. *Tumour Biol* 2016; 37: 5063–5074.
 42. Zhang W, Hou T, Niu C, et al. B3GNT3 expression is a novel marker correlated with pelvic lymph node metastasis and poor clinical outcome in early-stage cervical cancer. *PLoS One* 2015; 10: e0144360.
 43. Ayhan A, Al RA, Baykal C, et al. Prognostic factors in FIGO stage IB cervical cancer without lymph node metastasis and the role of adjuvant radiotherapy after radical hysterectomy. *Int J Gynecol Cancer* 2004; 14: 286–292.
 44. Stock RG, Chen AS and Karasek K. Patterns of spread in node-positive cervical cancer: the relationship between local control and distant metastases. *Cancer J Sci Am* 1996; 2: 256–262.
 45. Wang W, Liu X, Meng Q, et al. Nomograms predicting survival and patterns of failure in patients with cervical cancer treated with concurrent chemoradiotherapy: a special focus on lymph nodes metastases. *PLoS One* 2019; 14: e0214498.
 46. Ma J, Zhao R, Wu YL, et al. Regional lymph node density-based nomogram predicts prognosis in nasopharyngeal carcinoma patients without distant metastases. *Cancer Imaging* 2023; 23: 123.
 47. Yang K, Tian J, Zhang B, et al. A multi-dimensional nomogram combining overall stage, dose volume histogram parameters and radiomics to predict progression-free survival in patients with locoregionally advanced nasopharyngeal carcinoma. *Oral Oncol* 2019; 98: 85–91.
 48. Jonska-Gmyrek J, Gmyrek L, Zolciak-Siwinska A, et al. Adenocarcinoma histology is a poor prognostic factor in locally advanced cervical cancer. *Curr Med Res Opin* 2019; 35: 595–601.
 49. Lou J, Zhang X, Liu J, et al. The prognostic value of radiological and pathological lymph node status in patients with cervical cancer who underwent neoadjuvant chemotherapy and followed hysterectomy. *Sci Rep* 2024; 14: 2045.
 50. Weidhaas JB, Li SX, Winter K, et al. Changes in gene expression predicting local control in cervical cancer: results from Radiation Therapy Oncology Group 0128. *Clin Cancer Res* 2009; 15: 4199–4206.
 51. Doddamani R and Chandra PS. Radiogenomics in neuro-oncology: a noninvasive way of understanding tumor biology. *Neurol India* 2024; 72: 698–699.
 52. Ferro M, Musi G, Marchioni M, et al. Radiogenomics in renal cancer management-current evidence and future prospects. *Int J Mol Sci* 2023; 24: 4615.